

Supporting Information

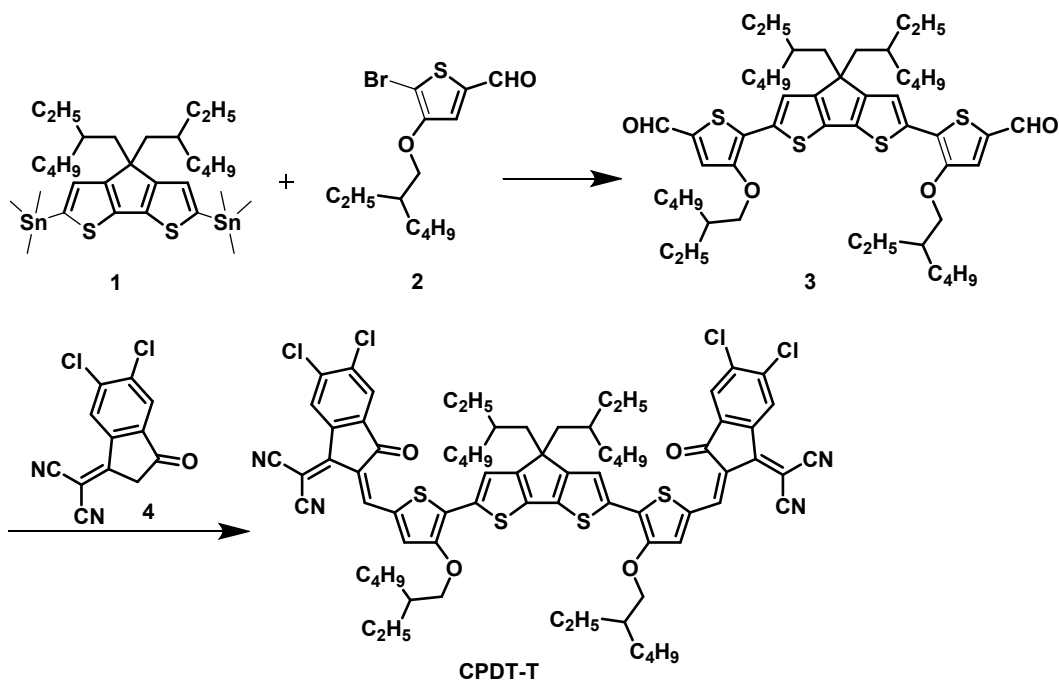
Materials

All reagents were purchased from commercial sources and used as received without further treatment. *N*-(carbonyl-methoxypolyethylene glycol 2000)-1,2-distearoyl-sn-glycerol-3-phosphoethanolamine sodium salt (DSPE-MPEG₂₀₀₀) were purchased from Aivituo (Shanghai) Pharmaceutical Technology Co., Ltd (shanghai, China). DMEM, fetal bovine serum (FBS), penicillin, and streptomycin were provided by GibcoBRL (Invitrogen Corp., CA, USA). *Staphylococcus aureus* (*S. aureus*) were purchased from BeNa Culture Collection (Henan, China).

Instruments

UV-vis-NIR absorption spectra were recorded on a UV/VIS/NIR Spectrometer LAMBDA750 (PerkinElmer, Inc, USA). Fluorescence emission was recorded on a Hitachi F-4600 fluorescence spectrophotometer (Hitachi, Tokyo, Japan). Particles size was measured using a Malvern Zeta Sizer Nano ZS90 (Malvern Instruments Co., UK). A FEI Tecnai G2 Spirit TWIN transmission electron microscope (Hillsboro, FL, USA) was used to obtain the transmission electron microscopy (TEM) images of the synthesized nanoparticles. The surface morphologies of bacteria were observed with field emission scanning electron microscopy (SEM) MERLIN Compact (ZEISS Deutschland, Germany). Infrared thermal images and temperature changes were recorded using a thermal imaging camera (TiS65, Fluke, Everett, WA, USA). The NIR laser (1064 nm) was purchased from Beijing Laserwave Optoelectronics Technology Co., Ltd. (LWIRPD-1064-20F, Laserwave, Beijing, China).

Synthesis of CPDT-T



Scheme S1 Synthetic routes to CPDT-T.

CPDT-T was synthesized based on the synthetic routes shown in Scheme S1. 1,1'-[4,4-Bis(2-ethylhexyl)-4H-cyclopenta[2,1-b:3,4-b']dithiophene-2,6-diyl]bis[1,1,1-trimethylstannane] (**1**) (1 g, 1.37 mmol), 5-bromo-4-[(2-ethylhexyl)oxy]-2-thiophene-carboxaldehyde (**2**) (1.09 g, 3.42 mmol) and Pd(PPh₃)₄ (79 mg, 0.068 mmol) were dissolved in anhydrous toluene (30 mL) under argon atmosphere. The resulting solution was stirred at 110 °C overnight. After cooling down to room temperature, the reaction mixture was poured into water (50 mL) and extracted with dichloromethane for three times (50 mL×3). The combined organic layers were dried over anhydrous Na₂SO₄ and filtered. The filtrate was concentrated under vacuum and purified by column chromatography on silica gel using petroleum ether/dichloromethane (v/v 1:1) as eluent to yield a red solid **3** (1.05 g, 87%). ¹H NMR (400 MHz, CDCl₃) δ 9.75 (s, 2H), 7.47 (s, 2H), 7.32 (s, 2H), 4.10 (d, *J* = 5.4 Hz, 4H), 1.95-1.81 (m, 6H), 1.67-1.58 (m, 6H), 1.56-1.47 (m, 2H), 1.43-1.33 (m, 8H), 1.25 (s, 2H), 1.03-0.85 (m, 28H), 0.72-0.60 (m, 12H).

Under the atmosphere of argon, the intermediate **3** (0.35 g, 0.40 mmol) and 2-(5,6-Dichloro-2,3-dihydro-3-oxo-1H-inden-1-ylidene)propanedinitrile (**4**) (0.33 g, 1.26 mmol) were dissolved in dry CHCl₃ (20 mL), and then pyridine (0.5 mL) was added to the mixture. After stirring and refluxing overnight, the mixture was cooled to room temperature and partial solvent was removed under vacuum. The residue was

added into 50 mL methanol dropwise. The precipitate was collected and further purified by silica gel using CHCl_3 as eluant to afford CPDT-T as a dark green solid (0.339 g, 63%). $^1\text{H NMR}$ (400 MHz, CDCl_3) δ 8.73 (d, $J = 6.7$ Hz, 4H), 7.98-7.86 (m, 2H), 7.64 (t, $J = 2.6$ Hz, 2H), 7.49 (s, 2H), 4.17 (d, $J = 5.2$ Hz, 4H), 2.04-1.86 (m, 6H), 1.74-1.56 (m, 8H), 1.51 (d, $J = 7.4$ Hz, 2H), 1.48-1.31 (br. s, 8H), 1.15-0.80 (m, 28H), 0.75-0.62 (m, 12H).

Preparation of CNP

CPDT-T (1.0 mg) in 1 mL THF was slowly injected into a solution of DSPE-MPEG₂₀₀₀ (5.0 mg) in DMSO (10 mL) under sonication. After that, the mixed solution was further kept in sonication for 15 min. The organic solvents were then removed by dialysis against Milli-Q water for 2 days (MW cutoff, 3.5 kDa). In the dialysis process, Milli-Q water was replaced approximately each 4 h. The resultant aqueous solutions containing nanoparticles were freeze-dried. The as-prepared CNP were stored in 4 °C freezer for the following usage.

Photothermal performance

CNP aqueous dispersions with different concentrations (0, 40, 90, 120, 180, 300 $\mu\text{g/mL}$) were irradiated with 1064 nm laser at a power density of 1.0 W/cm^2 for 17 min to evaluate the effect of CNP concentration on the photothermal performance. Similarly, CNP aqueous dispersions (180 $\mu\text{g/mL}$) were also irradiated with 1064 nm laser at different power densities (0.3, 0.5, 0.8, 1.2, 1.5, 2.0 W/cm^2) for 17 min to check the effect of laser power densities on the photothermal performance of CNP. During these tests, the temperature was recorded at intervals of 30 seconds with a thermal imaging camera (TiS65, Fluke, Everett, WA, USA).

Photothermal conversion efficiency

CNP aqueous dispersions (180 $\mu\text{g/mL}$) were irradiated by 1064 nm laser at 1.0 W cm^{-2} for 17 min, and then the solution was cooled down naturally to ambient temperature. The temperature of the solution was recorded at intervals of 30 s during this process. The photothermal conversion efficiencies (η) can be calculated referring to the following Equation (1):

$$\eta = \frac{hS(T_{max} - T_{Surr}) - Q_{Dis}}{I(1 - 10^{-A})} \quad (1)$$

Where h represents the heat transfer coefficient, S is the surface area of the container, T_{\max} represents the maximum steady-state temperature, T_{Surr} is the ambient temperature of the environment, Q_{Dis} represents the heat dissipation from the light absorbed by the solvent and the quartz sample cell. I indexes laser intensity (1.0 W cm^{-2}), and A is the absorbance of the sample at 1064 nm. hS can be calculated referring to the following Equation (2):

$$\tau = \frac{m_D c_D}{hS} \quad (2)$$

Where m_D and c_D index the solution mass and heat capacity (4.2 J/g) of pure water used as the solvent, respectively. As noted, τ can be calculated referring to the following Equation (3):

$$t = \tau \ln\left(\frac{T_{RT} - T_{\text{Surr}}}{T_{\max} - T_{\text{Surr}}}\right) \quad (3)$$

where T_{RT} denotes as the real-time temperature in the cooling period, τ is calculated to be 497.78 s for CNP from the linear regression of the cooling time of the material and the negative natural logarithm of θ (Fig. 3E and 3F).

In vitro antibacterial activity

The antibacterial efficiency of CNP was evaluated using a spread plate method. *S. aureus* were cultured in fresh medium for 17 h on a $37 \text{ }^\circ\text{C}$ (170 r/min) constant temperature shaker. A $100 \text{ }\mu\text{L}$ aliquot of *S. aureus* solution was mixed with $100 \text{ }\mu\text{L}$ different concentrations of CNP solution ($0, 40, 90, 120, 180, 250 \text{ }\mu\text{g/mL}$) and fresh medium ($800 \text{ }\mu\text{L}$) in a glass tube. The above solution was placed in dark at $37 \text{ }^\circ\text{C}$ for 2 h. Then, two sets of the *S. aureus* suspensions treated with CNP were kept in the dark or irradiated by 1064 nm laser at 1.2 W cm^{-2} for 8 min. Finally, all of the *S. aureus* suspensions were serially diluted 1×10^6 folds with water. A $100 \text{ }\mu\text{L}$ portion of the dilution with bacteria was spread on the solid agar plate. The plates were cultured at $37 \text{ }^\circ\text{C}$ for 16 h. The number of bacteria was counted by a counter. The inhibition ratio was determined by calculating the number of colony-forming units (CFU). The CFU ratio was calculated according to the following equation:

$$CFU \text{ Ratio} = \frac{C}{C_0} \times 100\%$$

Where C is the CFU of the experimental group treated with CNP under NIR irradiation, and C_0 is the CFU of the control group.

Morphological observation of bacteria

After treating bacteria in the same way as described in vitro antibacterial experiments, the samples were centrifuged (3000 rpm, 5 min) and washed with water. The precipitate was fixed with 2.5% glutaraldehyde for 12 h at 4 °C, subsequently, glutaraldehyde was removed. The mixture was washed twice with water, dehydrated with different gradients of ethanol (30%, 50%, 70%, and 90%, 10 min). 10 μ L of the suspension was dropped on a silicon wafer. After drying overnight, the specimens were coated with gold before SEM measurements.

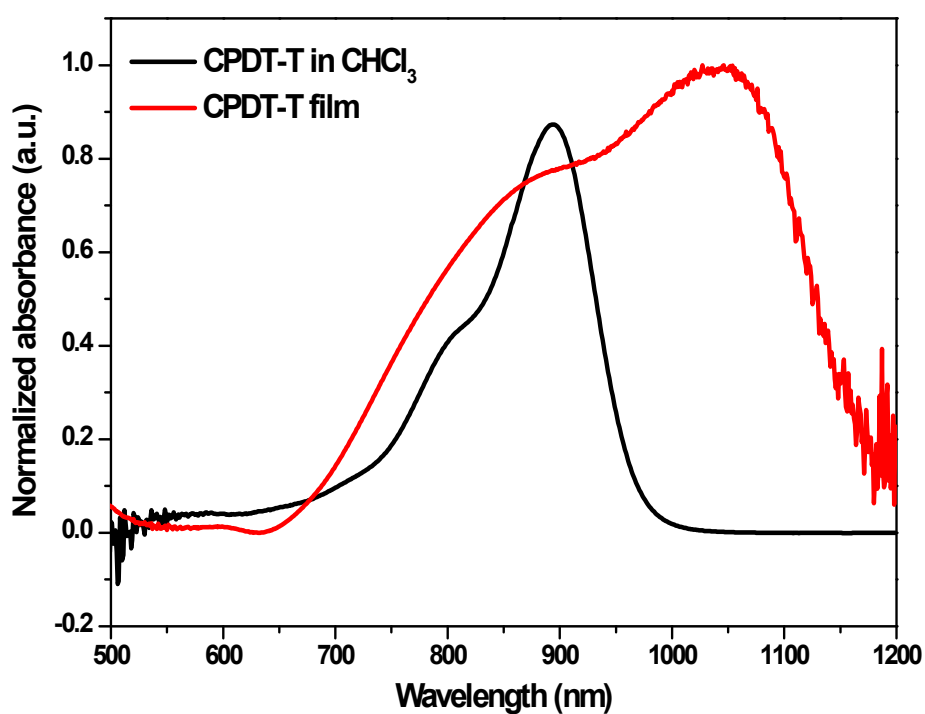


Fig. S1 Absorption spectra of CPDT-T in dilute chloroform and film state.

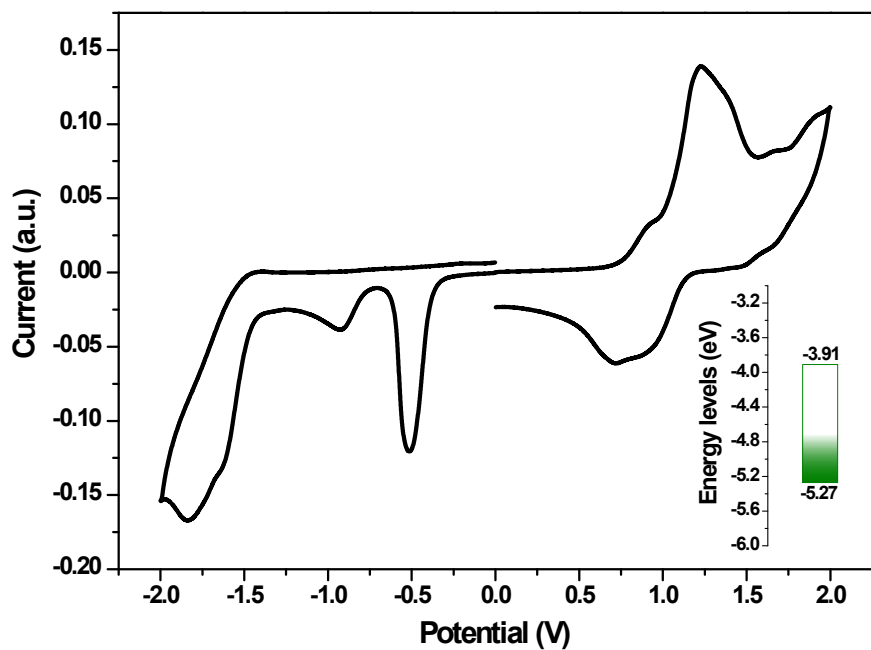


Fig. S2 CV curves of CPDT-T film.

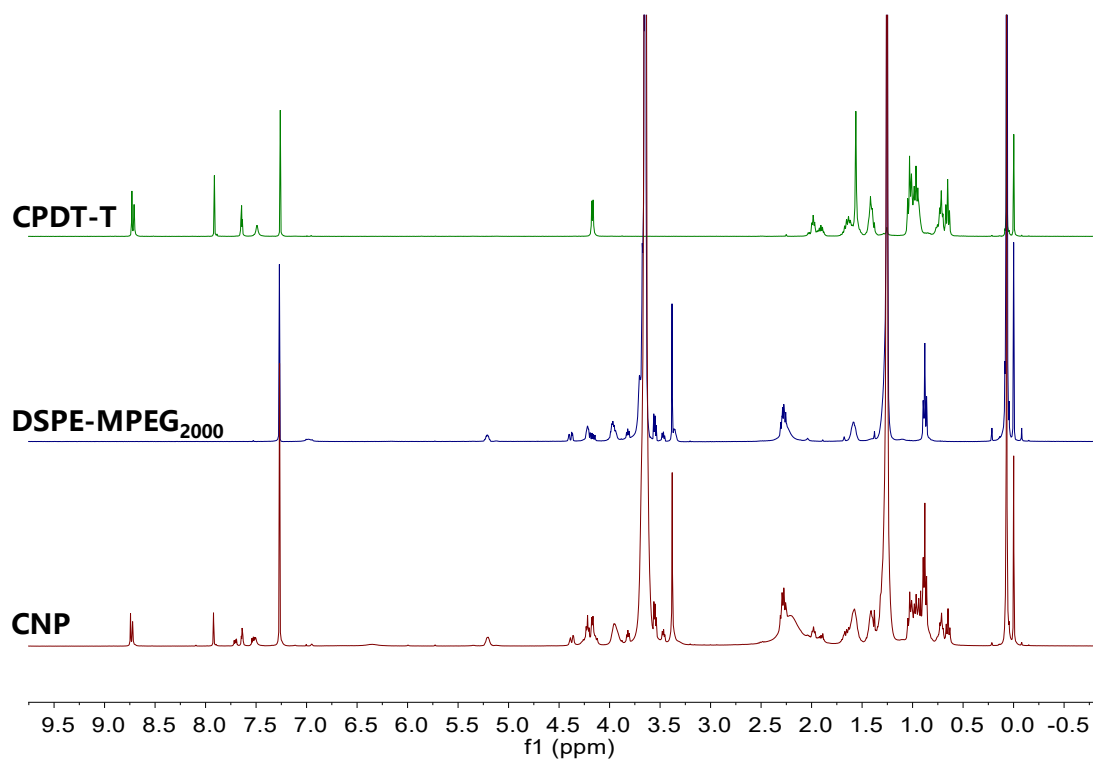


Fig. S3 ¹H NMR spectra of CPDT-T, DSPE-MPEG₂₀₀₀ and nanoparticles CNP.

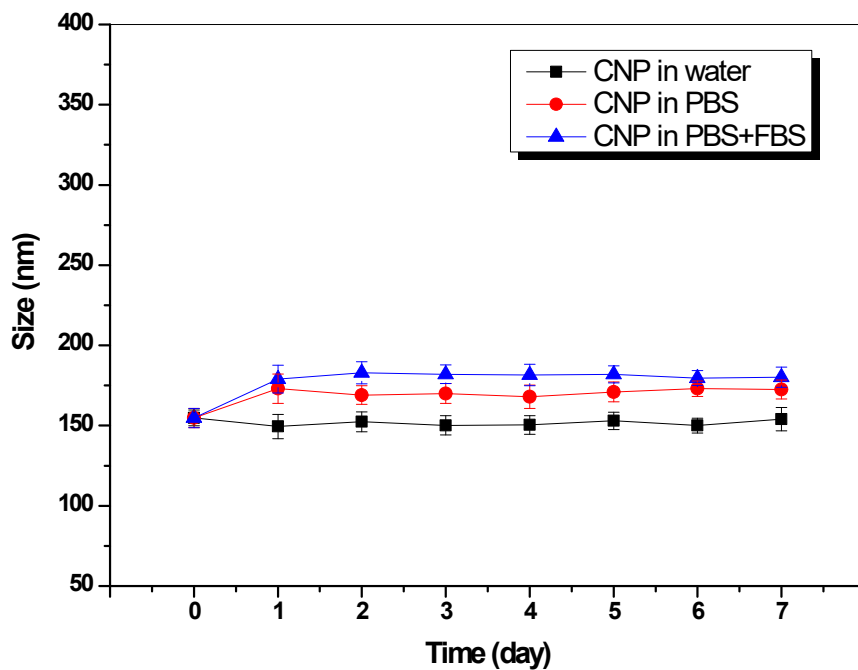


Fig. S4 Size change of CNP (300 µg/mL) in water, PBS, and PBS+ fetal bovine serum (FBS) with storage time.

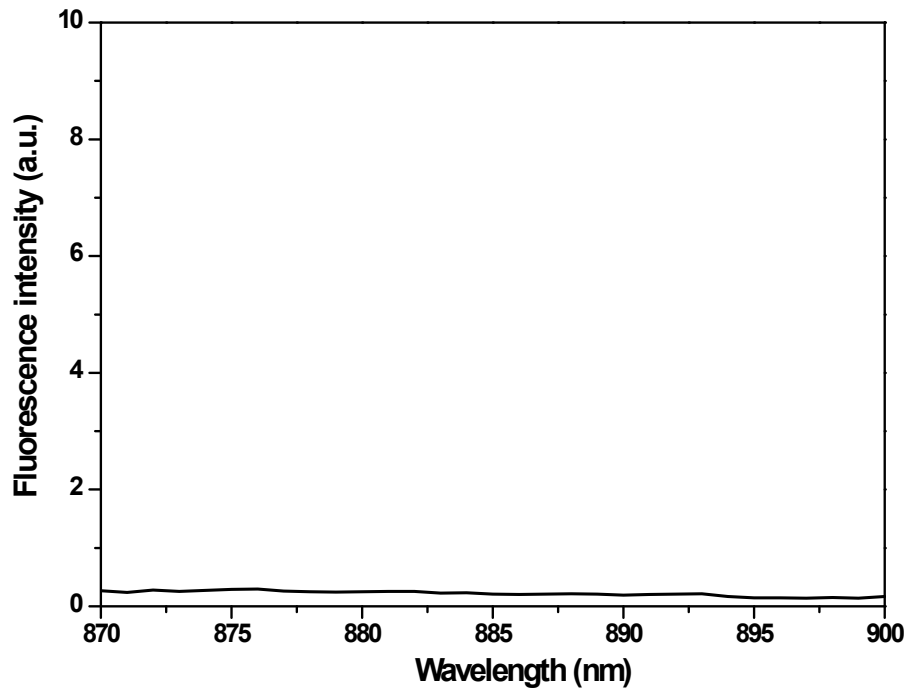


Fig. S5 Fluorescent spectrum of CNP aqueous dispersions (180 µg/mL).

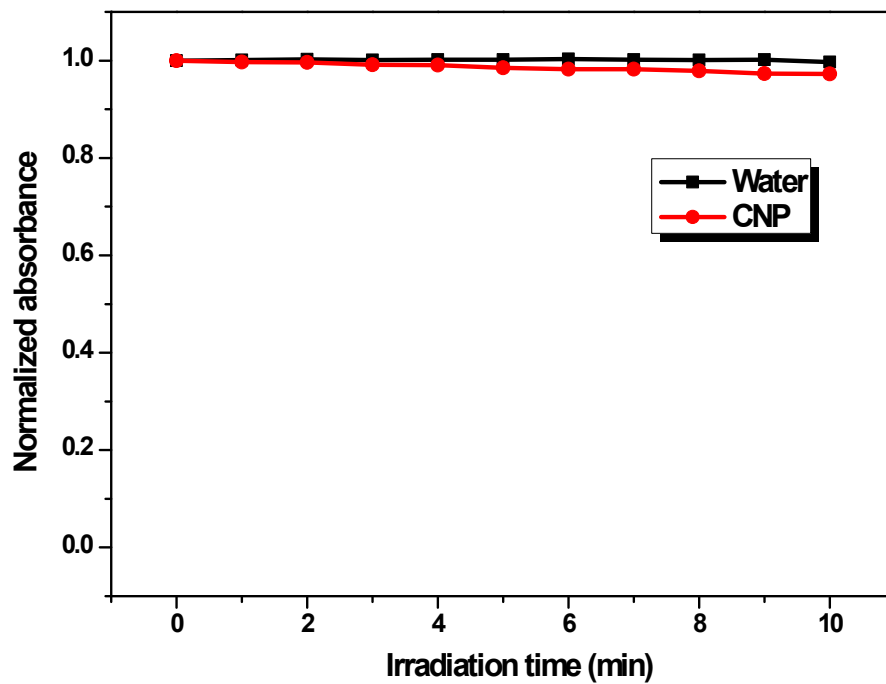


Fig. S6 Changes of absorbance at 415 nm of DPBF in presence of CNPs (180 $\mu\text{g/mL}$) under 1064 nm laser irradiation at 1.0 W/cm^2 with time.

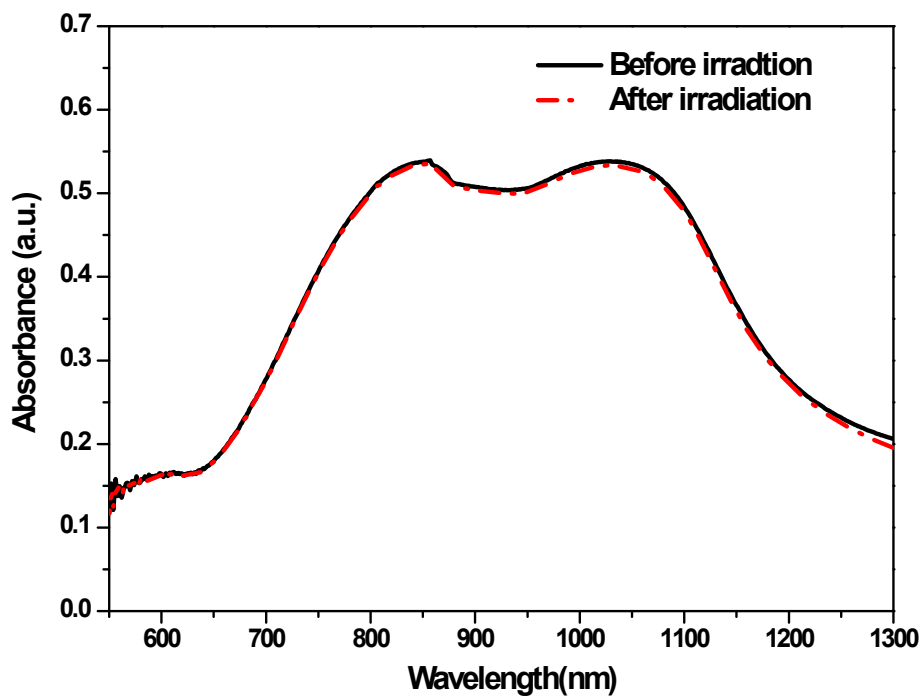


Fig. S7 Absorption spectra of CNP before and after NIR laser irradiation.

Table S1 Summary of the NIR-II organic nanomaterials for PTT therapy under 1064 nm laser irradiation

Names	Laser irradiation	PTCE (%)	Application	Ref.
TBDOPV-DT NPs	1064 nm (0.9 W/cm ²)	50	Anti-tumor	[1]
SPNs2	1064 nm (0.5 W/cm ²)	35	Anti-tumor	[2]
Lip (DPQ+2DG)	1064 nm (1.0 W/cm ²)	40.92	Anti-tumor	[3]
Lip(PTQ/GA/AIPH) NPs	1064 nm (1.0 W/cm ²)	42.15	Anti-tumor	[4]
OSPN12	1064 nm (1.0 W/cm ²)	45.25	Anti-tumor	[5]
PpCTLNPs	1060 nm (1.0 W/cm ²)	58	Anti-tumor	[6]
PSQPNs-DBCO	1064 nm (1.0 W/cm ²)	33.4	Anti-tumor	[7]
PEDOT:ICG@PEG-GTA	1064 nm (1.5 W/cm ²)	71.1	Anti-bacteria	[8]
TTQ-2TC NPs	1064 nm (1.0 W/cm ²)	34.9	Anti-tumor	[9]
BAF3 NPs	1064 nm (0.75 W/cm ²)	47	Anti-tumor	[10]
BAF4 NPs	1064 nm (0.75 W/cm ²)	80	Anti-tumor	[10]
IT-SS NPs	1064 nm (1.0 W/cm ²)	77	Anti-tumor	[11]
BH 990	1064 nm (2.0 W/cm ²)	45.7	Anti-tumor	[12]
BH 1024	1064 nm (2.0 W/cm ²)	41.3	Anti-tumor	[12]
PER-TCNQ NP	1064 nm (1.0 W/cm ²)	42	Anti-bacteria	[13]
CNP	1064 nm (1.2 W/cm ²)	49	Anti-bacteria	this work

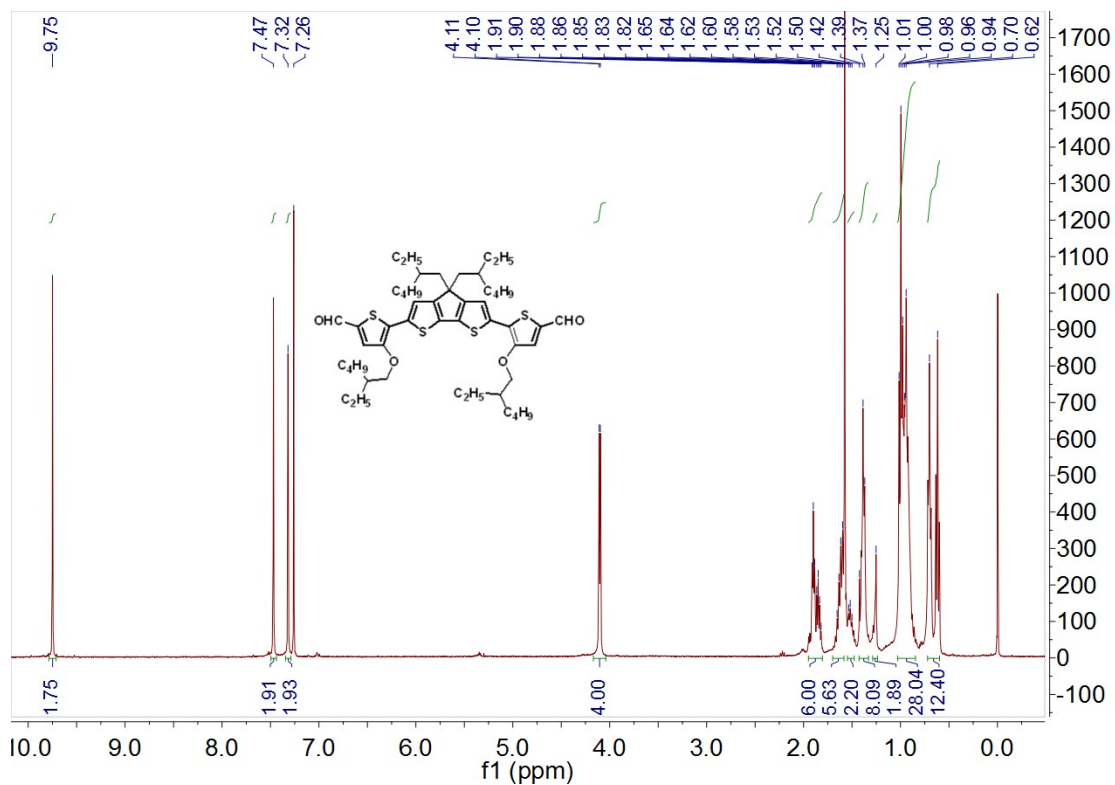


Fig. S8 ^1H NMR spectrum of compound 3.

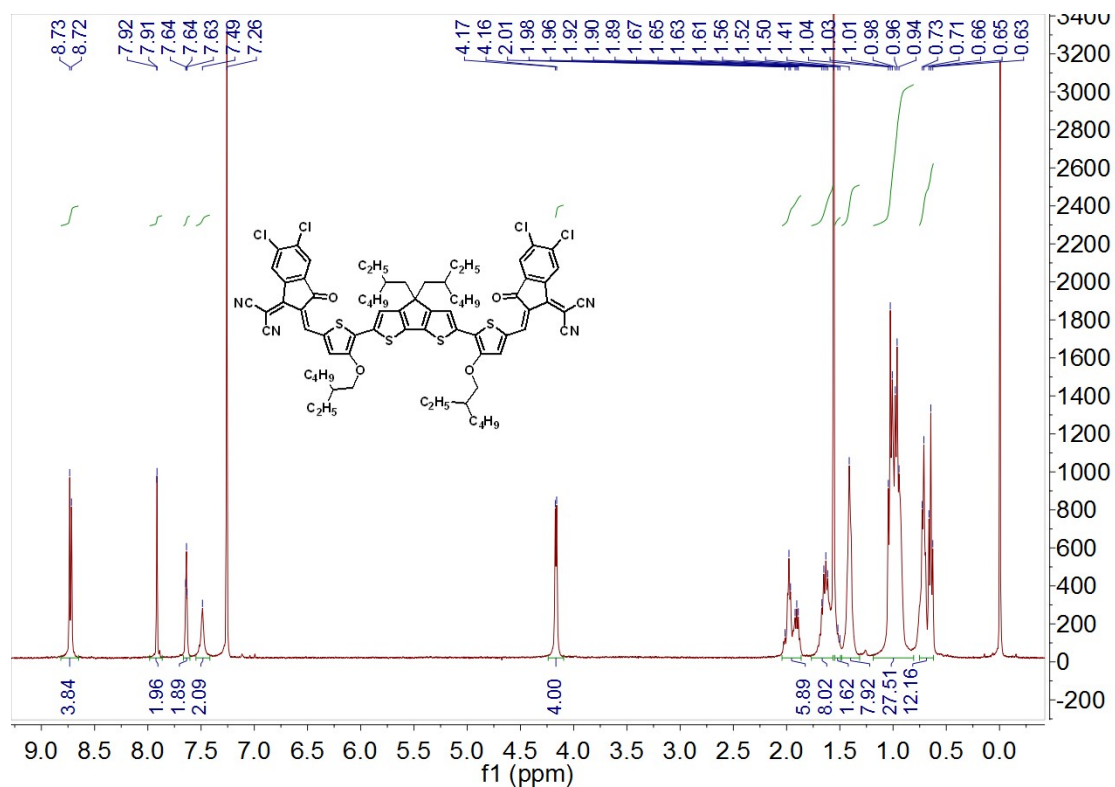


Fig. S9 ^1H NMR spectrum of CPDT-T.

References

- [1] T. Sun, J. H. Dou, S. Liu, X. Wang, X. Zheng, Y. Wang, J. Pei and Z. Xie, *ACS Appl. Mater. Interfaces*, 2018, **10**, 7919-7926.
- [2] W. Zhang, X. Sun, T. Huang, X. Pan, P. Sun, J. Li, H. Zhang, X. Lu, Q. Fan and W. Huang, *Chem. Commun.*, 2019, **55**, 9487-9490.
- [3] Y. Dai, Z. Sun, H. Zhao, D. Qi, X. Li, D. Gao, M. Li, Q. Fan, Q. Shen and W. Huang, *Biomaterials*, 2021, **275**, 120935.
- [4] Y. Dai, H. Zhao, K. He, W. Du, Y. Kong, Z. Wang, M. Li, Q. Shen, P. Sun and Q. Fan, *Small*, 2021, **17**, 2102527.
- [5] C. Yin, H. Zhang, B. Sun, S. Chen, X. Jiang, X. Miao, P. Sun, W. Hu, Q. Fan and W. Huang, *Adv. Funct. Mater.*, 2021, **31**, 2106575.
- [6] X. Zhang, Y. Yang, T. Kang, J. Wang, G. Yang, Y. Yang, X. Lin, L. Wang, K. Li, J. Liu and J. S. Ni, *Small*, 2021, **17**, 2100501.
- [7] W. Zhang, W. Deng, H. Zhang, X. Sun, T. Huang, W. Wang, P. Sun, Q. Fan and W. Huang, *Biomaterials*, 2020, **243**, 119934.
- [8] L. Li, Y. Liu, P. Hao, Z. Wang, L. Fu, Z. Ma and J. Zhou, *Biomaterials*, 2015, **41**, 132-140.
- [9] X. Song, X. Lu, B. Sun, H. Zhang, P. Sun, H. Miao, Q. Fan and W. Huang, *ACS Appl. Polym. Mater.*, 2020, **2**, 4171-4179.
- [10] Z. Jiang, C. Zhang, X. Wang, M. Yan, Z. Ling, Y. Chen and Z. Liu, *Angew. Chem. Int. Ed.*, 2021, **60**, 22376-22384.
- [11] S. Li, Q. Deng, Y. Zhang, X. Li, G. Wen, X. Cui, Y. Wan, Y. Huang, J. Chen, Z. Liu, L. Wang and C. S. Lee, *Adv. Mater.*, 2020, **32**, 2001146.
- [12] H. Bian, D. Ma, X. Zhang, K. Xin, Y. Yang, X. Peng and Y. Xiao, *Small*, 2021, **17**, 2100398.
- [13] S. Tian, H. Bai, S. Li, Y. Xiao, X. Cui, X. Li, J. Tan, Z. Huang, D. Shen, W. Liu, P. Wang, B. Z. Tang and C. S. Lee, *Angew. Chem. Int. Ed.*, 2021, **60**, 11758-11762.